JOURNAL OF Applied Polymer SCIENCE

Thermal Response of an Electric Heating Rapid Heat Cycle Molding Mold and Its Effect on Surface Appearance and Tensile Strength of the Molded Part

Guilong Wang,[1,2] Guoqun Zhao,[1,2] Yanjin Guan[1,2]

[1]Key Laboratory for Liquid-Solid Structural Evolution and Processing of Materials (Ministry of Education), School of Materials Science and Engineering, Shandong University, Jinan, Shandong 250061, People's Republic of China

[2]Engineering Research Center for Mold & Die Technologies, School of Materials Science and Engineering, Shandong University, Jinan, Shandong 250061, People's Republic of China

Correspondence to: G. Zhao (E-mail: zhaogq@sdu.edu.cn; guoqun_zhao@yahoo.com)

ABSTRACT: Rapid heat cycle molding (RHCM) is a newly developed injection molding technology in recent years. In this article, a new electric heating RHCM mold is developed for rapid heating and cooling of the cavity surface. A data acquisition system is constructed to evaluate thermal response of the cavity surfaces of the electric heating RHCM mold. Thermal cycling experiments are implemented to investigate cavity surface temperature responses with different heating time and cooling time. According to the experimental results, a mathematical model is developed by regression analysis to predict the highest temperature and the lowest temperature of the cavity surface during thermal cycling of the electric heating RHCM mold. The verification experiments show that the proposed model is very effective for accurate control of the cavity surface temperature. For a more comprehensive analysis of the thermal response and temperature distribution of the cavity surfaces, the numerical-method-based finite element analysis (FEA) is used to simulate thermal response of the electric heating RHCM mold during thermal cycling process. The simulated cavity surface temperature response shows a good agreement with the experimental results. Based on simulations, the influence of the power density of the cartridge heaters and the temperature of the cooling water on thermal response of the cavity surface is obtained. Finally, the effect of RHCM process on surface appearance and tensile strength of the part is studied. The results show that the high-cavity surface temperature during filling stage in RHCM can significantly improve the surface appearance by greatly improving the surface gloss and completely eliminating the weld line and jetting mark. RHCM process can also eliminate the exposing fibers on the part surface for the fiber-reinforced plastics. For the high-gloss acrylonitrile butadiene styrene/polymethyl methacrylate (ABS/PMMA) alloy, RHCM process reduces the tensile strength of the part either with or without weld mark. For the fiber-reinforced plastics of polypropylene (PP) + 20% glass fiber, RHCM process reduces the tensile strength of the part without weld mark but slightly increases the tensile strength of the part with weld mark. © 2012 Wiley Periodicals, Inc. J. Appl. Polym. Sci. 000: 000–000, 2012

KEYWORDS: molding; manufacturing; theory and modeling; fibers; morphology

Received 24 April 2012; accepted 29 June 2012; published online
DOI: 10.1002/app.38274

INTRODUCTION

Rapid heat cycle molding (RHCM) is a newly developed injection molding technique in recent years, which can greatly improve surface appearance of the part. Unlike the constant mold temperature control strategy by circling coolant through cooling channels in conventional injection molding (CIM), a dynamic mold temperature control strategy based on rapid mold heating and cooling is introduced in RHCM. According to mold temperature variation, a complete RHCM cycle can be divided into four stages including rapid heating, high-temperature holding, rapid cooling, and low-temperature holding, as depicted in Figure 1. At the beginning of RHCM process, the mold cavity surfaces will be rapidly heated to a relatively high temperature, generally higher than the glass transition temperature of the plastic material. At the following high-temperature holding stage, the polymer melt is injected out through the nozzle and runner system to fill mold cavity. After the mold cavity has been completely filled, the injection mold will be rapidly cooled to solidify the shaped polymer melt in the mold cavity. After that, at the following low-temperature holding stage, the injection mold is opened to take out the molded part.

As the cavity surface temperature during filling process in RHCM is much higher than that in CIM, the premature solidification of the polymer melt and the resulting frozen layer in

Applied Polymer SCIENCE

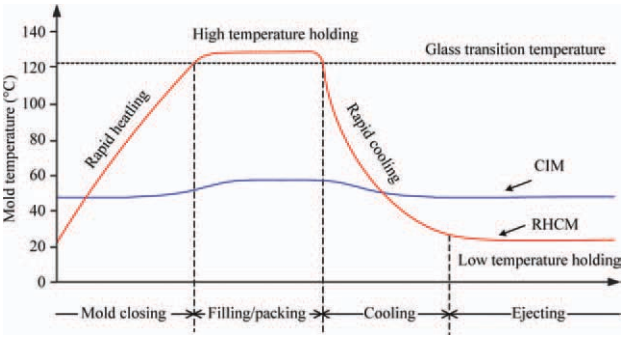

Figure 1. Comparison of mold temperature variation in RHCM and CIM. [Color figure can be viewed in the online issue, which is available at wileyonlinelibrary.com.]

CIM can be greatly alleviated or even completely eliminated in RHCM. As a consequence, the mobility of the polymer melt, especially the melt close to the cavity surface, can be greatly improved and the filling resistance can also be significantly reduced by RHCM. Therefore, RHCM has the potentiality to be used to improve part surface appearance by eliminating the surface defects such as flow mark, weld mark, jetting mark, and so forth, and increasing part surface gloss.[1–4] Additionally, it can also be used to reduce the residual stress of the molded part[5,6] and increase the flow length of the polymer melt so as to mold the thin wall part or the part with microfeatures.[7–10] Although RHCM has many technical advantages over CIM, it is not an easy work to achieve a rapid and uniform heating and cooling of the injection mold, especially for the large-scale mold or the mold with complicated cavity surfaces, taking into account such a short injection molding cycle, usually in a few seconds to tens of seconds. In fact, the most critical technique for RHCM is how to heat and cool the cavity surfaces rapidly and uniformly within a relatively short molding cycle time so as to not only improve the part quality but also ensure high production efficiency.

In the past decade, researchers have developed various kinds of rapid heating and cooling systems for injection mold temperature control in RHCM. Kim et al.[11] developed a momentary mold surface heating process in which the gas flame was used to heat the mold cavity surfaces. As the combustion reaction of the gas fuel and the oxygen will release large amount of heat in a very short time, the cavity surfaces can be heated rapidly. However, it is difficult to achieve a precise control of the cavity surface temperature due to the poor controllability of the combustion process. Furthermore, flame heating will bring more insecurity issues for injection production and the flame may also damage the cavity surfaces of injection mold. Yao and Kim[12] developed a rapid heating and cooling system consisting of one metallic heating layer and one oxide insulation layer for RHCM. The oxidation and heating layers with very thin thickness are, respectively, coated on the metallic mold base with the outer surfaces of the metallic heating layer as the cavity surfaces. When two charged electrodes are applied on the metallic heating layers, the heating layer will be heated by joule heat owing to the passage of the electric current through itself. As the metallic heating layer has a very low heat capacity, the heating layer or the cavity surfaces can be heated rapidly. Although the cavity surfaces can be rapidly heated and cooled with such rapid heating and cooling system, the low thermal strength of the coated layers leads to a low mold service life, which limits its application in actual injection molding production. Chen et al.[13,14] used electromagnetic induction heating and coolant cooling to rapidly heat and cool the mold cavity surfaces. In mold heating, a specially designed copper coil passing high-frequency current is placed near the cavity surfaces to induce eddy current in the mold. The joule heat resulting from the eddy current will then raise the mold temperature. Because of the so-called skin-effect of the high-frequency electromagnetic induction, the induced eddy current will confine at the mold surfaces. Therefore, only a very thin layer of the mold metal will be heated and hence the cavity surface can be heated rapidly. The major drawback of induction heating is that it is very difficult to embed the induction coil inside the mold and accordingly an external drive and control system should be used to precisely control the movement and placement of the induction coil. Furthermore, the induction coil should be carefully designed according to the cavity geometry so as to achieve a uniform heating of the cavity surface. Chang and Hwang[15] developed a rapid heating system to make use of infrared heating method to directly heat the mold cavity surfaces. The infrared heating system is very similar to the induction heating system, but the induction coil in the former one is changed into the halogen lamps in the latter one. Experimental studies have shown that the cavity surface can also be rapidly heated. However, it is very difficult to achieve a uniform heating of the cavity surface because of the low design flexibility of the infrared heating device. Chen et al.[16] designed a gas-assisted heating system to make use hot gas to heat the cavity surfaces directly. Although the cavity surfaces can also be rapidly heated, the hot gas channel should be carefully designed to achieve a uniform heating of the cavity surfaces.

In the above several rapid heating and cooling systems, the mold cavity surfaces are all directly heated and hence they all have relatively high heating efficiency. However, because of various technical problems or shortcomings, these systems for direct heating of cavity surfaces are still not widely used in actual production at present. In fact, the most easiest and economical methods for mold heating are to pass the hot medium through the heating channels or embed electric heat elements in the mold so as to heat the cavity surfaces from the inside of the injection mold. In this common heating method, the whole mold cavity plates need to be heated first to raise the cavity surface temperature indirectly. As the mold cavity plates, especially for the large injection mold, usually have a high heat capacity due to their large volume, it is difficult to achieve a rapid thermal response of the cavity surfaces. Therefore, such indirect heating methods based on hot medium or heaters are generally considered to be time-consuming and energy-consuming. However, our previous studies have shown that these indirect heating methods can also provide competitive heating and cooling rates of the cavity surfaces with optimal mold and heating/cooling systems design.[17–19] The production efficiency of RHCM

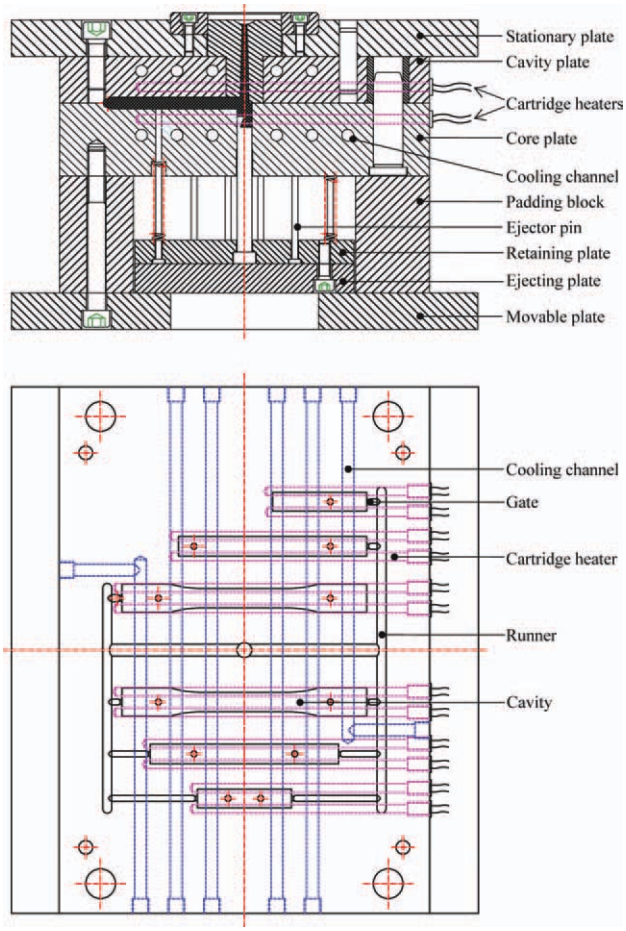

Figure 2. The two-dimensional structure of the RHCM mold with electric heating. [Color figure can be viewed in the online issue, which is available at wileyonlinelibrary.com.]

based on these indirect or inner heating methods can reach or even surpass that of CIM. Kang[20] presented an electric heating mold with a separate heating cavity plate. The whole cavity plate is heated by the heating elements mounted in the back surface of the cavity plate. For this electric heating mold, the thickness of the cavity plate should be thin enough to achieve rapid heating of the cavity surface.

In this study, a new RHCM mold with electric heating and coolant cooling is developed. Experiment design is conducted to investigate the thermal response of the cavity surfaces. Mathematical models are developed by regression analysis to evaluate and predict temperature response of the cavity surface temperature during thermal cycling process. Heat transfer simulations are also conducted using the computer aided engineering (CAE) software of ANSYS thermal modules to investigate the temperature distribution and thermal response of the cavity surfaces. The simulation results are compared with the experimental results to evaluate the simulation accuracy. The effect of power density of the cartridge heaters on heating efficiency and the effect of coolant temperature on cooling efficiency are investigated based on thermal response simulations. The feasibility of the electric heating mold for application in RHCM is evaluated. Finally, process experiments are implemented with the developed electric heating mold to investigate the effect of RHCM process on surface appearance and tensile strength of the part.

EXPERIMENTS AND NUMERICAL SIMULATIONS

RHCM Mold with Electric Heating

The two-dimensional structure of the electric heating RHCM mold is shown in Figure 2. The RHCM mold has six cavities that are used to mold the standard specimens with and without weld marks. The dimensions of the specimens for tensile tests, impact tests, and heat deflection tests are designed according to ASTM D638, ASTM D256, and ASTM D648, respectively. To achieve a balance filling of the cavities, filling analysis is conducted using the commercial software of Moldflow MPI to optimize the runner systems. After optimization, all the cavities can be fully filled almost at the same time, as shown in Figure 3.

The heating system of the RHCM mold consists of 24 cartridge heaters, which are embedded symmetrically in the stationary cavity plate and the movable cavity plate. The cartridge heaters typed MCHPA are supplied by MISUMI (China) Precision Machinery Trading. The diameters and nominal power densities of all the cartridge heaters are 6 mm and 15 W/cm^2, respectively.

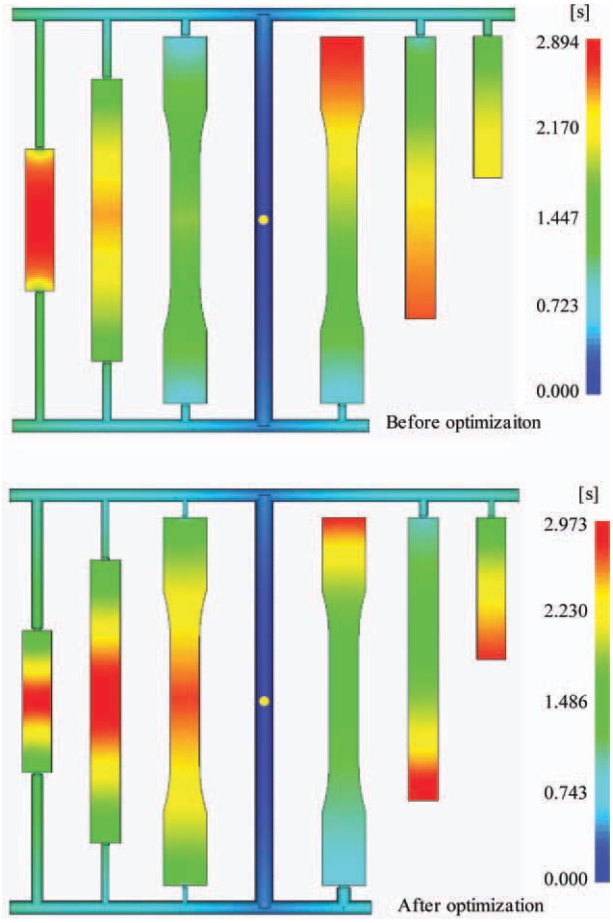

Figure 3. Comparison of the filling process before and after runner system optimization. [Color figure can be viewed in the online issue, which is available at wileyonlinelibrary.com.]

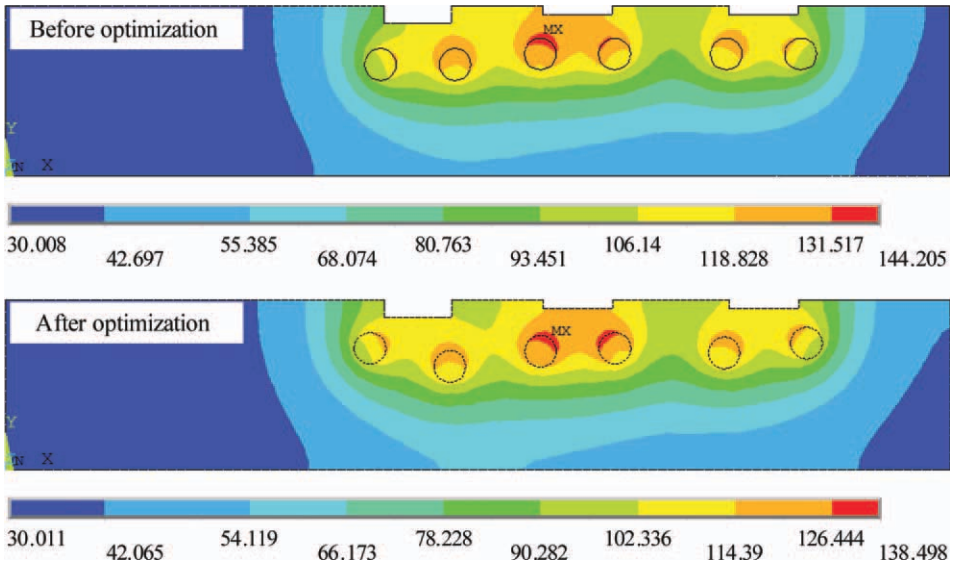

Figure 4. Comparison of cavity surface distributions in heating process before and after optimization of the positions of the cartridge heaters (Unit: °C). [Color figure can be viewed in the online issue, which is available at wileyonlinelibrary.com.]

The total nominal power of all the cartridge heaters is 11,960 W. To achieve a uniform heating of each cavity surface, the location of the cartridge heaters in the cavity plate is optimized based on CAE analysis. The comparison of the temperature distributions in the cavity plate before and after optimization is shown in Figure 4. After optimization, the cavity surface can be heated much more uniformly. The cooling system of the RHCM mold consists of several parallel cooling channels in the stationary and movable cavity plates. The diameter of the cooling channel is 8 mm and the average distance between adjacent cooling channels is 16 mm. The average distance from the center of the cooling channel to the cavity surfaces is 20 mm, which is about two times of the distance from the center of the heater to the cavity surface. To improve the structural strength and stiffness of the cavity plates, the cooling channels are placed perpendicularly to the cartridge heaters, as shown in Figure 5.

Thermal Response Measurements of the Cavity Surfaces

A data acquisition system is developed to measure and record the temperature response of the cavity surfaces in thermal cycling process of RHCM. The whole data acquisition system is composed of thermal couples, thermal data logger, computer, and the corresponding data processing program, as shown in Figure 6. Thermocouples are connected to the thermocouple data logger through compensation wires. The thermocouple data logger is then connected to personal computer (PC) through a USB RS232 cable. To accurately sense the rapid temperature variety of the cavity surfaces, a fast-response and adhesive type thin film thermocouple ST-50 supplied by Nippon Rika Kogyosho is used. The response time (to reach 95% of the steady-state temperature) and time constant (to reach 63% of the steady-state temperature) of the thermocouple are 0.4 s and 0.04 s, respectively. For each sample cavity, a thermocouple will be pasted on its surface. The positions of the thermocouples are shown in Figure 7. The thermocouple data logger USB TC-08 is provided by Pico Technology in UK. With accompanying the data processing program of PicoLog, the cavity surface temperatures can be recorded and displayed through PC.

In thermal response experiments, each thermal cycle of the mold can be divided into four stages: heating, high-temperature holding, cooling, and low-temperature holding. In heating stage, all the cartridge heaters in the cavity plate will be turned on to heat all the six cavities. In high-temperature holding stage, all the cartridge heaters will be turned off to stop heating. In cooling stage, the corresponding cooling pipes will be opened to pass the cooling water into the cooling channels to cool the cavity rapidly. The measured temperature and velocity of the cooling water are about 20°C and 2.94 m/s, respectively. In low-temperature holding stage, the cooling water will be cut off to stop cooling and the residual cooling water in the cooling channels will be blown out by the compressed air for preparation of the next heating stage. To investigate the effect of the heating time and cooling time on temperature responses of the cavity surfaces, a two factor full-factorial experiment design is used, as listed in Table I. The heating time has six levels that are 10, 20, 30, 40, 50, and 60 s. The cooling time has five levels that are 20, 30, 40, 50, and 60 s. The high-temperature holding time and

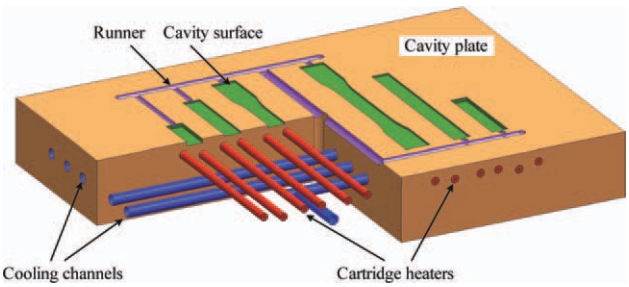

Figure 5. The layout of the cooling channels and cartridge heaters in the cavity plate. [Color figure can be viewed in the online issue, which is available at wileyonlinelibrary.com.]

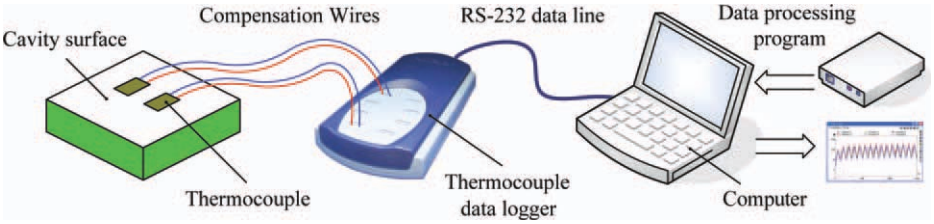

Figure 6. The data acquisition system for measuring thermal response of the cavity surfaces. [Color figure can be viewed in the online issue, which is available at wileyonlinelibrary.com.]

low-temperature holding time are both set to 10 s. During the whole experiments, the environment temperature changes very little and fluctuates between 25 and 27°C.

Thermal Response Simulation of Electric Heating RHCM Mold

The numerical model for thermal response simulation is shown in Figure 8. The thermal and physical properties of the related materials are given in Table II. In thermal response simulation, the mold heating time, high-temperature holding time, mold cooling time, and low-temperature holding time are assumed to 60, 10, 50, and 10 s, respectively.

The initial temperature of the model is equal to the ambient temperature of 25°C. The heat transfer mode between the outer surfaces of the mold and the surrounding environment is free air convection. Accordingly, the convective heat transfer coefficient is assumed to be 15 W/m^2 °C.[21] In heating stage, heat flux is loaded on the contact surfaces between the inner ceramic mandrels and the ceramic fillers of the cartridge heaters to simulate heating of the heaters. The calculated heat flux values for cartridge heaters from left to right in Figure 8 are 16.12, 16.12, 13.74, 13.50, 13.93, 13.72, 13.77, 13.77, 13.46, 12.80, 13.63, and 13.71 W/cm^2, respectively, which are calculated according to the measured power of the heater in experiments. In cooling stage, the heat transfer mode at the inner surfaces of the cooling channels is forced convective heat transfer. The calculated convective heat transfer coefficient according to cooling channel diameter, cooling water properties, and cooling water flow velocity is 11,741 W/m^2 °C.[21] Based on the above initial and boundary conditions, thermal responses of the electric heating mold in the first two thermal cycles are simulated.

Additionally, to investigate the power density of the cartridge heaters on the heating efficiency and the temperature of the cooling water on cooling efficiency, a series of thermal response simulations are performed. In these simulations, the power density of the cartridge heaters is assumed to have four levels including 10, 15, 20, and 30 W/cm^2, and the cooling water temperature is assumed to have three levels including 10, 20, and 30°C.

Experiments of RHCM Process

Two types of plastics are used in experiments. One is a type of high-gloss ABS/PMMA (RS-300 HF) produced by KINGFA Sci. & Tech. Its melt flow rate, density, and glass transition temperature are 14 g/10 min (220°C/10 kg), 1.15 g/cm^3 (23°C), and 107°C. The other one is a type of fiber-reinforced plastic, PP + 20% glass fiber (GP2201F), produced by LG Chemical. Its melt flow rate, density, and glass transition temperature are 24 g/10 min (220°C/10 kg), 1.06 g/cm^3 (23°C), and 135°C. Before injection molding, the materials will be dried at 85°C for 8 h. After predrying, the materials will be injection molded both with CIM process and RHCM process. In CIM process, the cavity surface temperature at the filling stage is about 36°C. In RHCM process, the cavity surface temperature at filling stage is about 118°C. Except the cavity surface temperature at the filling stage, the other injection molding parameters in RHCM are the same with those in CIM. The processing parameters for the two materials are given in Table III.

Based on the developed electric heating RHCM mold and the corresponding dynamic mold temperature control system, the experiments are performed on a horizontal injection molding machine (XL-680) produced by Ningbo Surely Meh. Its maximum clamping force, maximum injection rate, maximum injection weight, and screw diameter are 680 kN, 75 cm^3/s, 116 g, and 33 mm.

An inverted metallographic microscope EPIPHOT200 produced by Nikon Japan is used to characterize the surface appearance and micrograph of the molded part. A portable gloss meter JFL-BZ60° produced by Tianjin JFL Technology is used to measure the part surface gloss according to ISO 2813. Tensile tests are performed on a CMT 4204 20 KN electrical testing machine at room temperature with the crosshead speed of 5 mm/min according to ASTM D638.

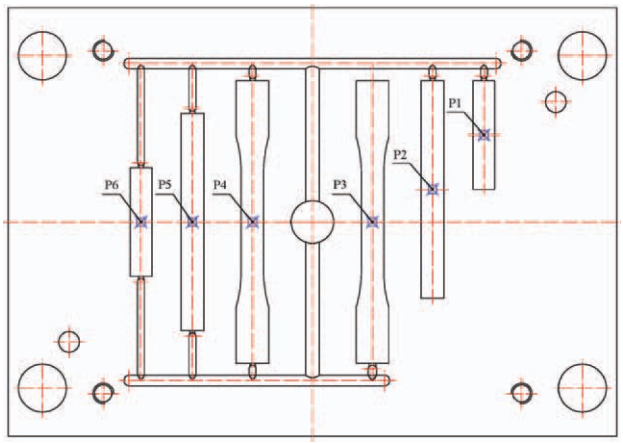

Figure 7. The positions of the thermocouples on cavity surfaces. [Color figure can be viewed in the online issue, which is available at wileyonlinelibrary.com.]

Table I. Factorial Experimental Design and Results

			P_1		P_2		P_3		P_4		P_5		P_6	
No.	t_h (s)	t_c (s)	T_{max} (°C)	T_{min} (°C)	T_{max} (°C)	T_{min} (°C)	T_{max} (°C)	T_{min} (°C)	T_{max} (°C)	T_{min} (°C)	T_{max} (°C)	T_{min} (°C)	T_{max} (°C)	T_{min} (°C)
1	10	20	56.2	40.7	62.2	44.9	53.9	44.2	59.0	46.1	63.7	50.0	55.8	45.6
2	10	30	50.8	33.9	56.1	37.3	48	36.96	52.79	38.49	56.7	41.4	50.1	38.3
3	10	40	48.1	30.3	52.8	33.1	44.9	32.9	49.4	34.1	52.8	36.2	46.9	34.0
4	10	50	45.4	27.6	49.7	29.7	42.0	29.6	46.2	30.7	49.2	32.2	43.8	30.5
5	10	60	44.3	26.0	48.2	27.5	40.5	27.5	44.5	28.5	47.5	29.7	42.6	28.4
6	20	20	85.3	55.5	94.0	63.2	81.3	62.2	89.6	65.5	98.8	71.8	84.9	63.8
7	20	30	76.5	43.9	84.5	50.5	71.6	49.8	79.5	52.6	87.6	57.3	75.5	51.5
8	20	40	71.9	37.6	79.0	43.0	66.3	42.6	73.7	44.7	81.0	48.3	70.1	43.9
9	20	50	67.2	32.9	73.6	37.1	61.2	36.9	68.0	38.7	74.6	41.3	64.8	38.0
10	20	60	65.5	30.1	71.5	33.4	58.8	33.3	65.5	34.9	72.1	36.8	62.7	34.3
11	30	20	110.0	68.2	119.0	79.0	104.6	77.3	114.5	82.1	127.2	90.0	109.5	79.1
12	30	30	98.5	52.7	106.5	61.8	91.8	60.9	101.1	64.7	112.7	70.6	97.2	62.6
13	30	40	90.4	43.3	97.7	50.8	83.1	50.3	91.7	53.3	102.3	57.8	88.5	51.8
14	30	50	88.5	38.3	95.1	44.5	80.3	44.3	88.5	46.9	99.1	50.3	85.9	45.5
15	30	60	85.4	34.0	91.7	38.9	76.4	38.8	84.4	41.1	94.7	43.6	82.1	39.9
16	40	20	134.5	80.5	142.9	94.6	128.1	93.0	139.1	98.6	154.5	108.0	134.5	95.0
17	40	30	118.9	61.2	126.5	73.0	111.0	72.0	121.2	76.8	135.9	83.8	117.7	73.5
18	40	40	109.1	49.4	116.1	59.2	100.5	58.6	109.9	62.5	123.5	67.7	107.4	60.0
19	40	50	105.1	42.7	111.4	50.6	95.4	50.4	104.3	53.7	117.9	57.8	102.5	51.6
20	40	60	102.4	37.7	108.3	44.1	91.7	44.1	100.4	46.9	113.9	50.0	99.1	45.2
21	50	20	149.4	87.9	157.4	104.1	142.2	102.3	152.4	107.9	170.6	118.6	149.9	104.1
22	50	30	136.0	67.9	142.4	81.9	126.6	80.9	137.5	86.4	154.3	94.1	134.7	82.6
23	50	40	126.9	55.4	133.2	67.4	116.6	66.9	126.6	71.3	143.3	77.3	124.8	67.9
24	50	50	123.2	47.6	128.7	57.5	112.0	57.3	121.9	61.4	138.2	66.0	120.7	58.5
25	50	60	117.1	40.9	122.2	48.7	105.0	48.7	114.2	52.1	130.4	55.6	113.6	49.8
26	60	20	163.5	95.6	172.8	114.6	157.5	112.6	166.4	118.6	187.3	129.5	165.0	113.5
27	60	30	151.5	74.2	157.4	90.6	141.6	89.6	152.1	95.6	171.2	104.3	150.6	91.4
28	60	40	140.7	59.9	146.7	74.0	130.5	73.6	140.8	78.7	159.0	85.1	139.2	74.8
29	60	50	136.2	50.8	143.0	63.1	125.8	63.0	135.9	67.4	154.4	72.3	135.1	64.0
30	60	60	130.5	44.0	135.3	53.2	117.9	53.4	127.5	57.1	145.8	60.7	127.1	54.2

RESULTS AND DISCUSSIONS

Thermal Response of the Electric Heating Mold

As shown in Table I, a total of 30 sets of experiments with different combinations of heating time and cooling are carried out to study the thermal responses of the cavity surfaces during thermal cycling process. Figure 9 shows some measured typical temperature response curves of the cavity surfaces. It can be found that the cavity surface temperatures are fluctuating around a gradually rising trend with the continuous thermal cycling process. After several thermal cycles, thermal responses of the cavity surfaces will reach a stable state. The longer the mold heating time or the shorter the mold cooling time, the more thermal cycles before reaching the stable thermal cycling state. For instance, only two thermal cycles are needed when the mold heating time is 20 s and the mold cooling time is 50 s; however, about 10 thermal cycles are needed when the mold

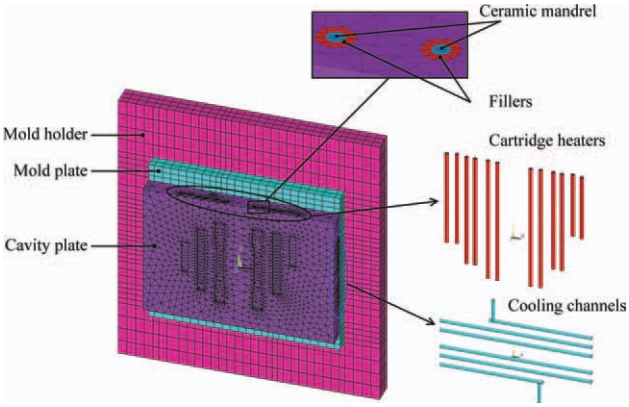

Figure 8. Thermal response simulation model of the electric heating mold. [Color figure can be viewed in the online issue, which is available at wileyonlinelibrary.com.]

Table II. Thermal and Physical Properties of the Mold Materials

Name	Material	Density (kg/m^3)	Thermal conductivity (W/m °C)	Capacity (J/kg °C)
Mold holder	HT 350	7800	47	440
Mold plate	AISI 1045	7850	43.4	473
Cavity plate	AISI H13	7800	24.3	460
Ceramic fillers	MgO-SiO_2	2700	5.5	1100
Ceramic mandrel	Al_2O3	3960	38	850

heating time is extended to 50 s and the mold cooling time is shortened to 20 s.

Both the maximum and minimum cavity surface temperatures during one thermal cycle depend on the mold heating time and mold cooling time. They can be increased by extending mold heating time or shortening mold cooling time or lowered by shortening mold heating time or extending mold cooling time. The maximum and minimum cavity surface temperatures after a stable thermal cycling process is achieved are logged in Table I. In the 30 sets of experiments, the maximum cavity surface temperature during thermal cycling process can exceed 185° with the mold heating time of 60 s and mold cooling time of 20 s.

Mathematical Model for Prediction of the Cavity Surface Temperature

The maximum and minimum cavity surface temperatures during thermal cycling process are two significant parameters for RHCM. The maximum cavity surface temperature has a great effect on the melt filling process, which is directly related to the surface quality of the molded part. A too low maximum cavity surface temperature will lead to low part quality, whereas a too high maximum cavity surface temperature will lead to energy waste and long molding cycle. The minimum cavity surface temperature has a great effect of the cooling of the molded part. A too low minimum cavity surface temperature will also lead to energy waste and long molding cycle, whereas a too high minimum cavity surface temperature will lead to inadequate cooling and hence warpage of the part. Therefore, an accurate control of the maximum and minimum cavity surface temperature is very significant in RHCM to ensure part quality, improve productivity, and reduce energy cost.

The effect of the mold heating time and cooling time on the maximum and minimum cavity surface temperatures at the cavity surface position of P_2 as depicted in figure 7 is shown in Figure 10. In Figure 10(a), it can be found that the mold heating time has a much more significant effect on the maximum cavity surface temperature than the mold cooling time. The maximum cavity surface temperature mainly depends on the mold heating time. In Figure 10(b), it can be found that the mold heating time and the mold cooling time both have very significant effect on the minimum cavity surface temperature. Anyway, the mold heating time and cooling time should be precisely controlled to achieve an accurate control of the cavity surface temperature. Generally, a thermocouple can be installed in the mold to feedback the cavity surface temperature, based on which the mold heating time and cooling time can be controlled indirectly. The drawback of this method is that the introduced thermocouple will result in cost increase of the mold design and manufacture. What's more, it is difficult for the thermocouple to sense the cavity surface temperature accurately without damaging the cavity surface.

Table III. Injection Molding Processing Parameters of the Two Materials

Parameters	ABS/PMMA	PP + 20% glass fiber
Melt temperature (°C)	230	230
Injection pressure (MPa)	50	60
Injection speed (cm^3/s)	26	30
Packing pressure (MPa)	45	50
Pacing time (s)	10	10

Besides the aforementioned method, the cavity surface temperature can be controlled by directly controlling the mold heating time and cooling time. However, the reasonable mold heating time and cooling time should be determined in advance according to the required maximum cavity surface temperature and minimum cavity surface temperature. To this end, mathematical models for numerically describing the relationship between the maximum and minimum cavity surface temperatures and the mold heating and cooling time are developed by regression based on the experimental results in Table I. The numerical prediction models for the maximum and minimum cavity surface temperatures are described with the following two equations, respectively.

$$T_{\max} = 59.2874 - 0.0152t_h^2 + 0.0149t_c^2 + 3.4230t_h - 1.5043t_c - 0.0108t_h t_c \quad (1)$$

$$T_{\min} = 60.8361 - 0.0048t_h^2 + 0.0191t_c^2 + 2.0839t_h - 1.8115t_c - 0.0215t_h t_c \quad (2)$$

With the two equations, the maximum and minimum cavity surface temperatures can be predicted conveniently based on the mold heating and cooling time. Moreover, the reasonable mold heating time and cooling time in RHCM process can also be obtained easily according to the required maximum and minimum cavity surface temperatures.

To verify the validity of the developed mathematical models, three sets of random experiments are performed. In the three sets of experiments, the required maximum cavity surface

Applied Polymer SCIENCE

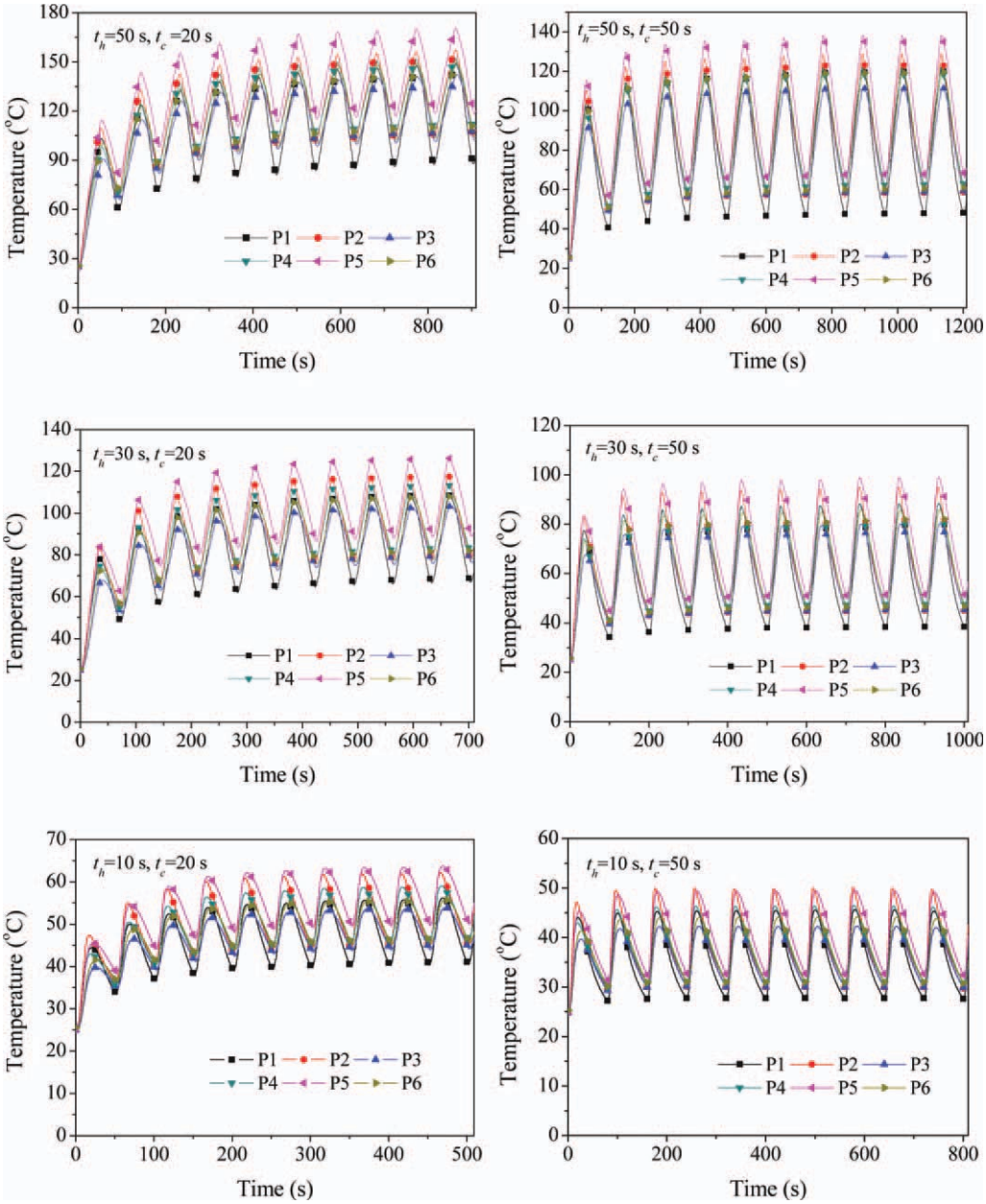

Figure 9. Some measured typical temperature responses of the cavity surfaces during thermal cycling experiments. [Color figure can be viewed in the online issue, which is available at wileyonlinelibrary.com.]

temperatures are assumed to 110, 130, and 90°C, respectively, and the required minimum cavity surface temperatures are assumed to 60, 70, and 50°C, respectively. By substituting the maximum and minimum cavity surface temperature into eqs. (1) and (2), the corresponding mold heating time and cooling time can be calculated. The calculated mold heating times for the three sets of experiments are 33.6, 44.6, and 24.5 s, respectively, and the calculated mold cooling times are 35.2, 35.5, and 35.6 s, respectively. Based on the calculated three sets of mold heating time and cooling time, thermal response experiments are conducted again to measure the temperature response of the cavity surface. Figure 11 shows the comparison of the required cavity surface temperature fluctuation ranges and the measured cavity surface temperature responses. It can be found that the measured maximum and minimum cavity surface temperatures in experiments are very consistent with the expected values. The maximum relative errors for the maximum and minimum cavity surface temperature in the three sets of experiments are only 3.1% and 2.8%, respectively. It demonstrates that the developed mathematical models can be used for the accurate control of the cavity surface temperature.

Temperature Distribution of the Cavity Surfaces During Heating and Cooling Process

For a comprehensive study of the temperature responses and distributions of the cavity surfaces in thermal cycling process,

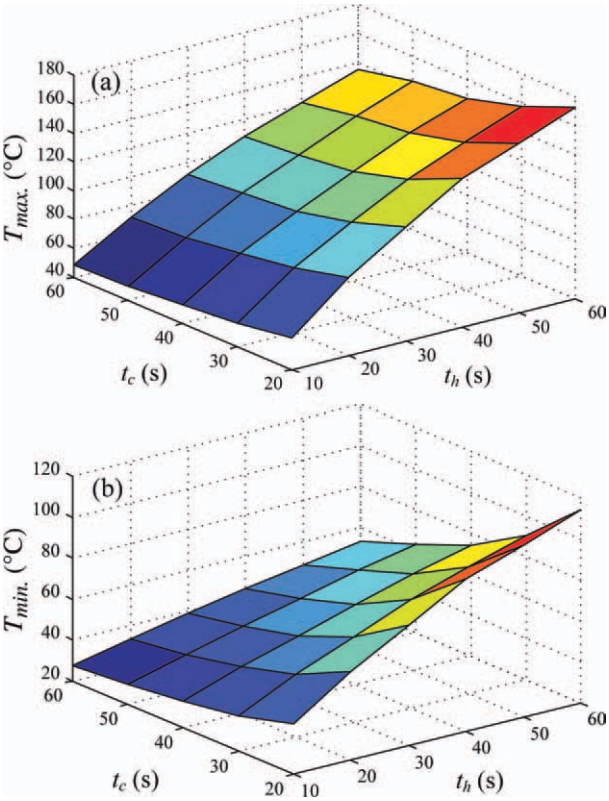

Figure 10. The effect of the mold heating time and cooling time on the maximum and minimum cavity surface temperatures: (a) the maximum cavity surface temperature and (b) the minimum cavity surface temperature. [Color figure can be viewed in the online issue, which is available at wileyonlinelibrary.com.]

thermal response of the electric heating RHCM mold in two continuous thermal cycles is simulated.

Figure 12 shows the temperature distributions of the electric heating RHCM mold at different stages and different times in two continuous thermal cycling processes. It can be found that the cavity surface temperatures for the thermal deflection specimens in the middle positions are higher than the cavity surface temperatures for the tensile and impact specimens at the edge positions, which is consistent with the experimental results. Additionally, the cavity surface temperature in the second thermal cycling process is higher than that in the first thermal cycling process. This phenomenon also has a good agreement with the experimental results shown in Figure 9. For each cavity, it can be seen from Figure 12 that the temperature distribution at the cavity surface is relatively uniform at different stages of the whole thermal cycling process. It indicates that the optimization design of the heating system during the electric heating RHCM mold design is very effective.

The comparison of the cavity surface temperature response curves obtained by experiments and simulations is shown in Figure 13. It is observed that the simulated temperature curves have a good agreement with the measured temperature curves. This verifies the validity of the simulation results further. It is noteworthy that the difference between simulation results and experimental results at the cooling stage is much larger than that in the heating stage. This is mainly because that the thermal contact resistances between different materials are neglected in simulation, which speeds up heat loss of the cavity surface.

Effect of the Power Density of Heating Elements on Heating Speed of the Cavity Surface

The temperature response curves of the cavity surface during heating stage corresponding to the cartridge heater with different power densities are shown in Figure 14. It is obviously

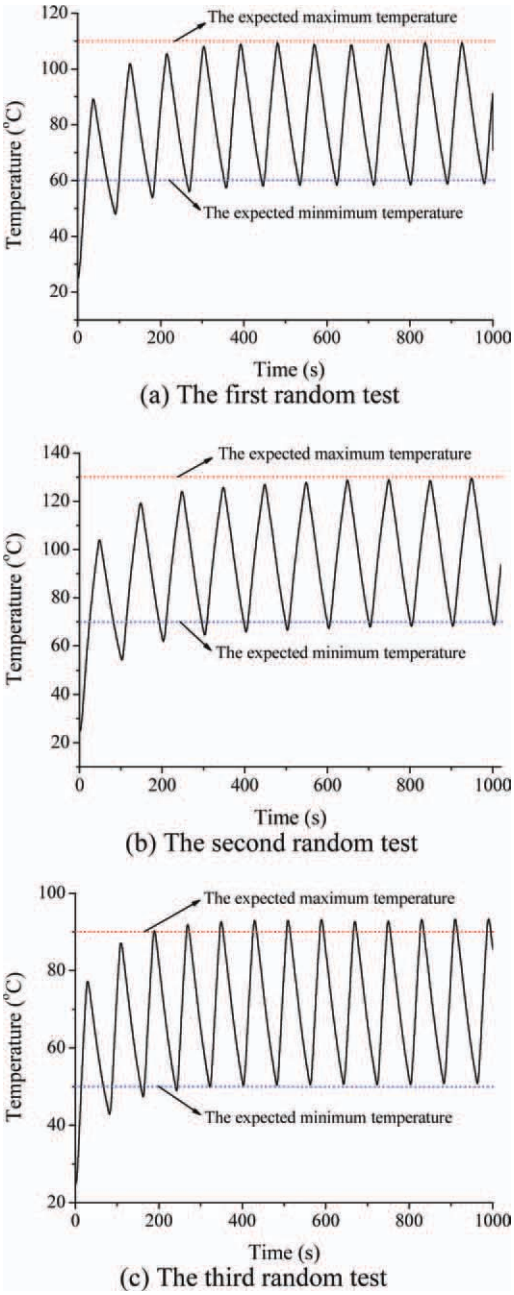

Figure 11. Comparison of the required cavity surface temperature fluctuation ranges and the measured cavity surface temperature responses. [Color figure can be viewed in the online issue, which is available at wileyonlinelibrary.com.]

Applied Polymer SCIENCE

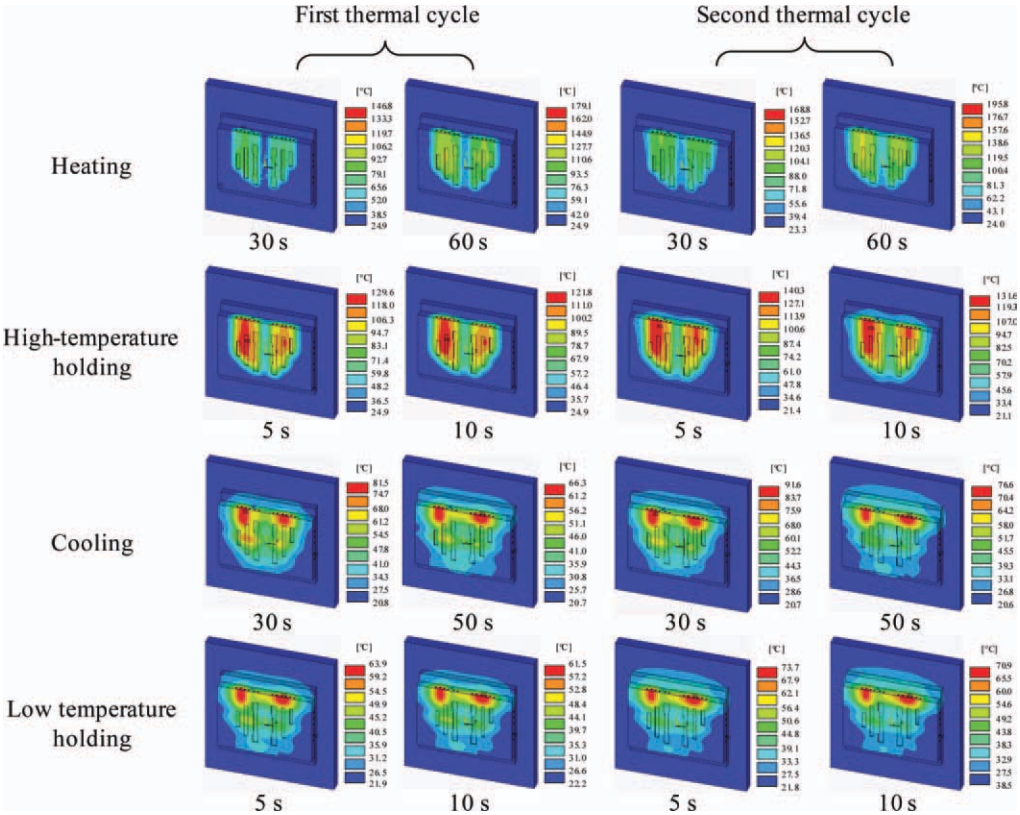

Figure 12. Temperature distributions of the electric heating RHCM mold at different stages and different times in two continuous thermal cycling processes. [Color figure can be viewed in the online issue, which is available at wileyonlinelibrary.com.]

illustrated that the heating speed of the cavity surface increases rapidly with the increase of the power density of the heaters. During the 60 s heating stage, the average temperature rise speed of the cavity surface for the cartridge heater with the power density of 10 W/cm^2, 15 W/cm^2, 20 W/cm^2, and 30 W/cm^2 are 1.20°C/s, 1.54°C/s, 2.40°C/s, and 3.60°C/s, respectively. It indicates that the power density of the heaters should be high enough to reduce the mold heating time and hence shorten the molding cycle of RHCM. For instance, the heating time for the cavity surface to be heated from 30 to 120°C can be reduced from 58 to 19 s when the power density of the heaters increases from 15 to 30 W/cm^2. Although the heating efficiency can be greatly improved by increasing power density of the heaters, the concept of "bigger is better" for the power density of the heaters is not quite right. First, it will be not helpful for shortening the

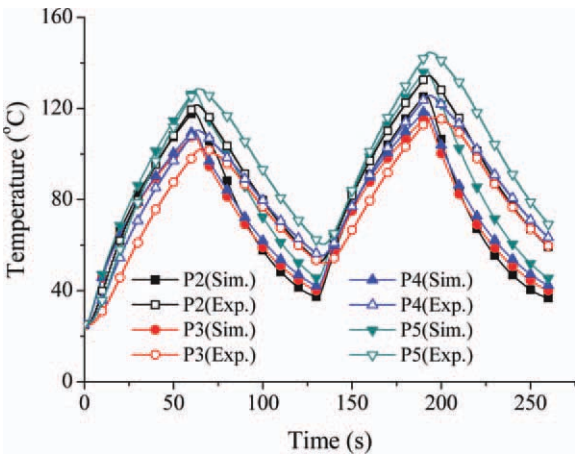

Figure 13. Comparison of the cavity surface temperature response curves acquired by simulations and experiments. [Color figure can be viewed in the online issue, which is available at wileyonlinelibrary.com.]

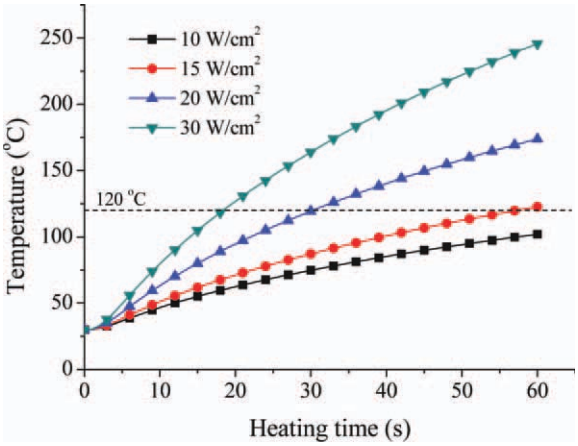

Figure 14. Temperature response curves of the cavity surface during heating stage corresponding to the heaters with different power density. [Color figure can be viewed in the online issue, which is available at wileyonlinelibrary.com.]

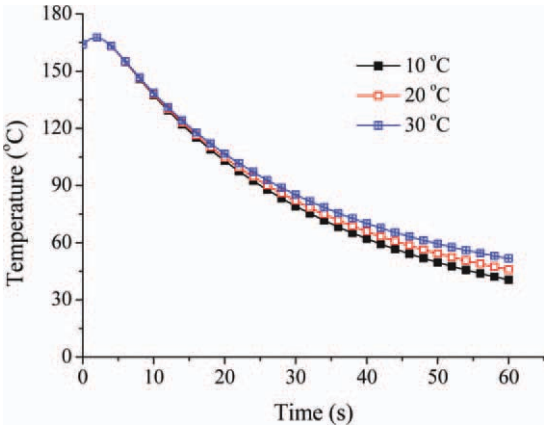

Figure 15. Temperature response curves of the cavity surface during cooling stage corresponding to cooling water with different temperatures. [Color figure can be viewed in the online issue, which is available at wileyonlinelibrary.com.]

injection molding cycle as the heating time reduces to a low enough level.[4] Second, the cost of the heater will increase dramatically with its power density increase. Third, the maximum power density of the cartridge heater has a certain upper limit due to technical reasons. At present, the maximum power density of the commercial cartridge heater is about 30 W/cm^2. Overall, the reasonable power density of the heaters in the RHCM mold should be decided by comprehensively considering the required heating time, the required cavity surface temperature, production cost, and so forth, of the RHCM process for a specific plastic product.

Besides the power density of the heaters, the layout of the heaters in the electric heating RHCM mold also has significant effect on the heating speed and temperature uniformity of the cavity surface. The optimization design of the heaters in RHCM mold is very necessary for a rapid and uniform heating the cavity surface, especially for the cavity with complicated geometries. The optimization design of the heaters will be studied in our future research work.

Effect of Cooling Water Temperature on Cooling Speed of the Cavity Surface

The temperature response curves of the cavity surface in cooling stage corresponding to cooling water with different temperatures are shown in Figure 15. It can be observed that there are very little differences between the three temperature response curves of the cavity surface. It indicates that the temperature of the cooling water has very limited effect on the cooling speed of the cavity surface. For cooling, the cavity surface temperature from160 to 65°C, the needed cooling times corresponding to the cooling water with temperature of 10°C, 20°C, and 30°C are 38 s, 40 s, and 45 s, respectively, which have no significant difference and are all in the acceptable level comparing with the cooling speed in CIM. Therefore, it can be concluded that the cooling water at the room temperature can meet the requirement of mold rapid cooling in RHCM and the chilled water with much lower temperature supplied by the specialized refrigeration equipment is not necessary by considering the reduction of energy consumption.

Effect of RHCM Process on Part Surface Appearance

Figure 16 shows the surface morphology comparison of the parts produced by CIM and RHCM. It is obviously illustrated

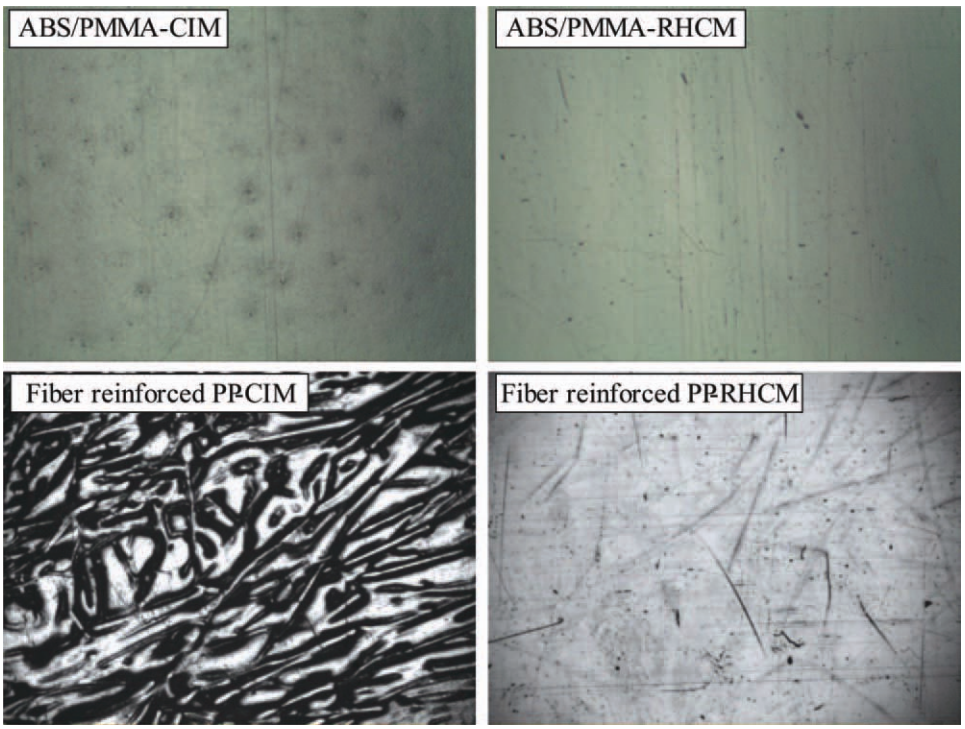

Figure 16. Surface morphology comparison of the parts produced with CIM and RHCM (×100). [Color figure can be viewed in the online issue, which is available at wileyonlinelibrary.com.]

Applied Polymer SCIENCE

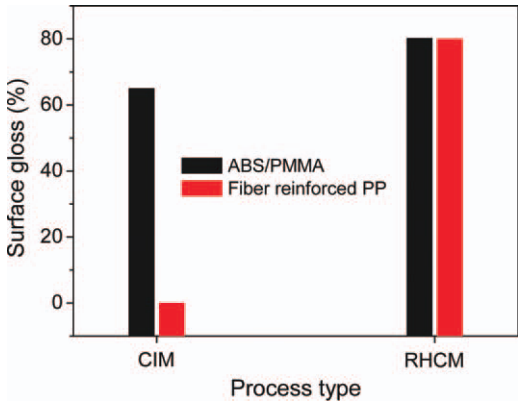

Figure 17. Surface gloss comparison of the parts produced with CIM and RHCM. [Color figure can be viewed in the online issue, which is available at wileyonlinelibrary.com.]

that the RHCM parts have much better surface appearance that CIM parts, especially for the fiber-reinforced plastics. In CIM, the premature cooling of the polymer melt during filling stage due to the relatively low mold cavity surface temperature makes the fibers exposed at the surface of the part, and hence the part surface is very rough. However, in RHCM, the much higher cavity surface during filling stage is able avoid the premature cooling of the polymer melt which can coat the glass fibers in it, and hence the exposed fibers on the part surface are eliminated absolutely. The surface gloss comparison of the parts produced with CIM and RHCM is presented in Figure 17. It can be found that the part surface gloss is significantly improved by RHCM. For the plastics of ABS/PMMA, the part surface gloss is increased from 65 to about 80%. For the glass fiber-reinforced PP, the part surface gloss is increased from 0 to about 80%.

The comparison of the surface morphology at the weld line region of the parts produced with CIM and RHCM is shown in Figure 18. It can be clearly seen that the weld line on RHCM part surface has disappeared completely. This is mainly because that the high-cavity surface temperature during filling stage significantly increases fluidity of the polymer melt and also the integration capacity of multistrand melts. For the same reason, RHCM is also able to eliminate the jetting mark on the part surface, as shown in Figure 19.

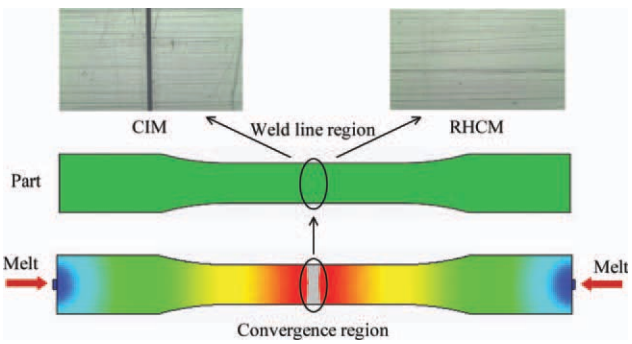

Figure 18. Comparison of the surface morphology at the weld line region of the parts produced with CIM and RHCM. [Color figure can be viewed in the online issue, which is available at wileyonlinelibrary.com.]

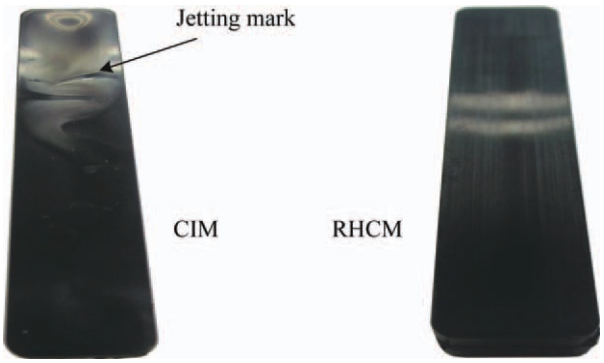

Figure 19. Comparison of the parts with jetting produced with CIM and RHCM.

Effect of RHCM Process on Part Strength

The tensile strength of the CIM and RHCM parts with and without the weld line is given in Figure 20. For the part without the weld line, the tensile strength of the part produced with CIM is higher than that of the part produced with RHCM. As the orientation of polymer chains in the plastic part is closely related to the tensile strength, the reduction of the tensile strength of the RHCM parts can be explained from the perspective of the degree of the polymer chain orientation in the following two aspects. First, the high-cavity surface temperature during filling stage in RHCM obviously reduces the flow resistance of the polymer melt and the shear stress suffered by the polymer melt also reduces accordingly. Therefore, the degree of the polymer chain orientation in RHCM parts will be less than that in CIM parts. Second, the oriented polymer chain after filling stage in RHCM can disorient much more enough that that in CIM due to the high-cavity surface temperature and relatively long cooling time. This also reduces the degree of polymer chain orientation in the final molded plastic part of RHCM. Because of the aforementioned two reasons, the polymer orientation along melt flow direction in RHCM parts is less than that in CIM parts. Therefore, the tensile strength of the RHCM part is lower than that of the CIM part.

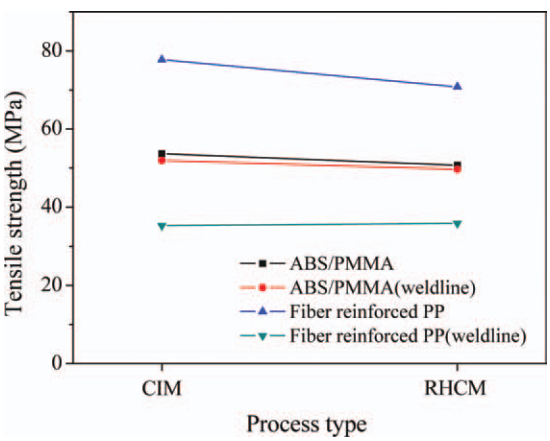

Figure 20. The tensile strength of the CIM and RHCM parts with and without the weld line. [Color figure can be viewed in the online issue, which is available at wileyonlinelibrary.com.]

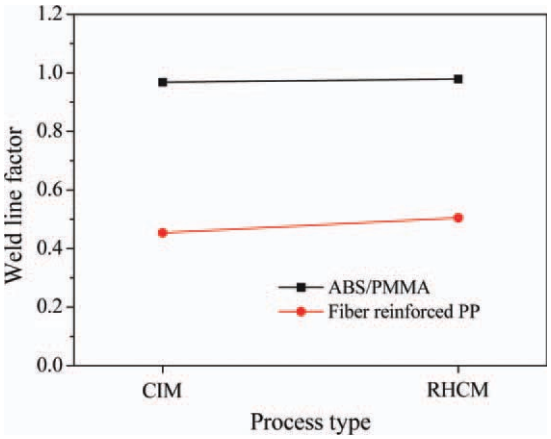

Figure 21. Comparison of the weld line factors for CIM and RHCM. [Color figure can be viewed in the online issue, which is available at wileyonlinelibrary.com.]

For the parts with the weld line, the tensile strength of the ABS/PMMA part molded with RHCM is lower than that of the ABS/PMMA part molded with CIM. However, for the fiber-reinforced PP, the weld line part molded with RHCM nearly has the same tensile strength with that molded with CIM. Such experimental results are quite opposite to the expected results, in which the weld line part molded with RHCM should be higher than that molded with CIM because the high-cavity surface temperature in RHCM can enhance the bond strength of multistrand polymer melts. The experimental results about the weld line strength in this study are also quite different from some previous experimental results by other researchers.[1] Their results show that the tensile strength can be greatly improved by RHCM process. However, some other research results confirm well with the present research results.[22] As the strength of weld line may be influenced by many other complicated factors besides the cavity surface temperature during filling process, further research works for the effect of RHCM process on weld line strength have to be done in future research work. The weld line factors (defined as the ratio between the strength of part containing a weld line and the strength of part without a weld line) for CIM and RHCM are shown in Figure 21. It can be clearly observed that the weld line factor for RHCM is much higher than that for CIM. This indicates that RHCM process can improve the weld line strength to a certain extent. Additionally, it is noteworthy that the weld line factor of the fiber-reinforced PP is much lower than that of the ABS/PMMA. This is because that the large number of glass fibers in the plastics obviously weakens the bond strength of multistrand polymer melts.

CONCLUSIONS

A new electric heating RHCM mold and the corresponding RHCM test production line based on it are developed in this article. Thermal responses of the electric heating RHCM mold are investigated by coupling experiments and numerical simulations. The effect of RHCM process on surface appearance and strength of the plastic part is investigated by a series of process experiments. The main conclusions of this work can be drawn as following:

1. The cavity surface temperature of the developed electric heating RHCM mold can be rapidly changed in a large temperature range during thermal cycling process of RHCM. The heating speed of the electric heating RHCM mold is very dependent on the power density of the heaters. Cooling water at the room temperature is sufficient to achieve a rapid cooling speed of the electric heating RHCM mold.
2. In thermal cycling process, the fluctuation of the cavity surface temperature of the electric heating RHCM mold is dependent on the mold heating time and the mold cooling time. The developed mathematic models can be used to effectively evaluate and predict the fluctuation range of the cavity surface temperature of the developed electric heating RHCM mold, which is very useful for process parameters settings of RHCM in experiments.
3. Compared with CIM process, RHCM process can greatly increase the surface gloss of the part, especially for the fiber-reinforced plastics. In addition, the exposed fibers, weld line, and jetting mark on the part surface can be completely eliminated by RHCM. Therefore, the parts molded with RHCM have much better surface appearance than those molded with CIM.
4. Compared with CIM process, RHCM process reduces the tensile strength of the part without weld line. For the plastics of ABS/PMMA, the tensile strength of the part with weld line is also slightly reduced by RHCM. However, for the plastics of fiber-reinforced PP, the tensile strength of the part with weld line is slightly increased by RHCM. The weld line factor can be improved with RHCM process both for ABS/PMMA and the 20% glass fiber-reinforced PP.

ACKNOWLEDGMENTS

The authors would like to acknowledge financial support from Program for Changjiang Scholars and Innovative Research Team in University of Ministry of Education of China under Grant No. IRT0931, Shandong Province High Technology Innovation Engineering Special Plan Program under Grant No. 2008ZZ10, and Program for New Century Excellent Talents in University under Grant No. NCET-08-0337.

REFERENCES

1. Chen, S. C.; Jong, W. R.; Chang, J. A. *J. Appl. Poly. Sci.* **2006,** *101*, 1174.
2. Wang, G. L.; Zhao, G. Q.; Li, H. P.; Guan, Y. *J. Polym. Plast. Technol. Eng.* **2009,** *48*, 671.
3. Park, K.; Sohn, D. H.; Cho, K. H. *J. Mech. Sci. Technol.* **2010,** *24*, 149.
4. Zhao, G. Q.; Wang, G. L.; Guan, Y. J.; Li, H. P. *Polym. Adv. Technol.* **2011,** *22*, 476.
5. Huang, M. S.; Tai, N. S. *J. Appl. Polym. Sci.* **2009,** *113*, 1345.
6. Park, K.; Kim, B.; Yao, D. G. *Polym. Plast. Technol. Eng.* **2006,** *45*, 903.

7. Yao, D. G.; Kim, B. *Polym. Plast. Technol. Eng.* **2002,** *41*, 819.
8. Chen, S. C.; Jong, W. R.; Chang, Y. J.; Chang, J. A.; Cin, J. C. *J. Micromech. Microeng.* **2006,** *16*, 1783.
9. Yu, M. C.; Young, W. B.; Hsu, P. M. *Mater. Sci. Eng. A Struct. Mater. Prop. Microstruct. Process.* **2007,** *460*, 288.
10. Chen, S. C.; Lin, Y. W.; Chien, R. D.; Li, H. M. *Adv. Polym. Technol.* **2008,** *27*, 224.
11. Kim, D. H.; Kang, M. H.; Chun, Y. H. *J. Injection Molding Technol.* **2001,** *5*, 229.
12. Yao, D. G.; Kim, B. *Polym. Eng. Sci.* **2002,** *42*, 2471.
13. Chen, S. C.; Jong, W. R.; Chang, J. A.; Chang, Y. J. *Int. Polym. Process.* **2006,** *21*, 457.
14. Chen, S. C. U.S.Pat. 7,060,952 (**2006**).
15. Chang, P. C.; Hwang, S. J. *J. Appl. Polym. Sci.* **2006,** *102*, 3704.
16. Chen, S. C.; Chien, R. D.; Lin, S. H.; Lin, M. C.; Chang, J. A. *Int. Commun. Heat Mass Transfer* **2009,** *36*, 806.
17. Wang, G. L.; Zhao, G. Q.; Guan, Y. J. *J. Appl. Polym. Sci.* **2010,** *119*, 902.
18. Wang, G. L.; Zhao, G. Q.; Li, H. P.; Guan, Y. J. *Mater. Design* **2010,** *31*, 3426.
19. Wang, G. L.; Zhao, G. Q.; Li, H. P.; Guan, Y. J. *Mater. Design* **2010,** *31*, 382.
20. Kang, M. H. *U. S. Pat. 7,670,539* (**2010**).
21. Wang, G. L. Ph.D. Dissertation, Shandong University, Jinan, Shandong, **2011.**
22. Xie, L.; Ziegmann, G. *Microsyst. Technol.: Micro Nanosyst. Inf. Storage Process. Syst.* **2009,** *15*, 1427.